DESY-01-122
TAUP - 2687 - 2001

DESY-01-122
TAUP - 2687 - 2001
August 29, 2001

Diffractive Dissociation and Saturation Scale from Non-Linear Evolution in High Energy DIS

E. Levin* [a),b)] and M. Lublinsky† [c),d)]

[a)] *HEP Department*
School of Physics and Astronomy
Raymond and Beverly Sackler Faculty of Exact Science
Tel Aviv University, Tel Aviv 69978, ISRAEL

[b)] *DESY Theory Group,*
D-22602, Hamburg, GERMANY

[c)] *Department of Physics*
Technion – Israel Institute of Technology
Haifa 32000, ISRAEL

[d)] *II. Institut für Theoretische Physik, Universität Hamburg*
Luruper Chaussee 149, 22761 Hamburg, GERMANY

August 29, 2001

arXiv:hep-ph/0108239 29 Aug 2001

Abstract

This paper presents the first numerical solution to the non-linear evolution equation for diffractive dissociation processes in deep inelastic scattering. It is shown that the solution depends on one scaling variable $\tau = Q^2/Q_s^{D\,2}(x, x_0)$, where $Q_s^D(x, x_0)$ is the saturation scale for the diffraction processes. The dependence of the saturation scale $Q_s^D(x, x_0)$ on both x and x_0 is investigated, ($Y_0 = \ln(1/x_0)$ is a minimal rapidity gap for the diffraction process). The x - dependence of Q_s^D turns out to be the same as of the saturation scale in the total inclusive DIS cross section. In our calculations $Q_s^D(x, x_0)$ reveals only mild dependence on x_0. The scaling is shown to hold for $x \ll x_0$ but is violated at $x \sim x_0$.

*e-mail: leving@post.tau.ac.il
†e-mail: mal@techunix.technion.ac.il

1 Introduction

Diffractive inclusive production in deep inelastic scattering (DIS) at high energy has become an area of particular interest of experts since it provides a deeper insight into dynamics of QCD in the kinematic region where the density of partons is expected to be high (see Ref.[1] and reference therein).

Inclusive diffraction in DIS offers an opportunity to probe the transition region between "soft" and "hard" interactions giving natural estimates for the value of the shadowing corrections in DIS, namely $\Delta F_2 = F_2 - F_2^{DGLAP} = F_D$ [1] as was firstly shown in Ref. [3] on the basis of the AGK cutting rules [4]. A more detail approach started with the Kovchegov-McLerran[5] formula which expresses the ratio of the diffraction cross section (σ_{diff}) to the total cross section (σ_{tot}) in DIS initiated by the quark-antiquark pair produced in $\gamma^* \to q + \bar{q}$ decay of the virtual photon. This formula reads

$$R = \frac{\sigma_{diff}}{\sigma_{tot}} = \frac{\int d^2 b \int dz \int d^2 r_\perp P^{\gamma^*}(z, r_\perp; Q^2)\, N^2(r_\perp, x; b)}{2 \int d^2 b \int dz \int d^2 r_\perp \; P^{\gamma^*}(z, r_\perp; Q^2)\; N(r_\perp, x; b)} \,. \tag{1.1}$$

where $N(r_\perp, x; b)$ is the imaginary part of the elastic dipole-target amplitude for dipole of the size $r_\perp$ scattered at fixed Bjorken $x = Q^2/W^2$ (Q^2 is the photon virtuality and W is its energy in the target rest frame) and at fixed impact b. $P^{\gamma^*}(z, r_\perp; Q^2)$ is the probability to find a quark-antiquark pair with size $r_\perp$ inside the virtual photon [6, 7]:

$$\begin{aligned} P^{\gamma^*}(z, r_\perp; Q^2) &= \frac{\alpha_{em} N_c}{2\pi^2} \sum_f Z_f^2 \sum_{\lambda_1, \lambda_2} \{\, |\Psi_T|^2 + |\Psi_L|^2 \,\} \qquad (1.2) \\ &= \frac{\alpha_{em} N_c}{2\pi^2} \sum_f Z_f^2 \{\, (z^2 + (1-z)^2) a^2 K_1^2(a\, r_\perp) + 4\, Q^2\, z^2 (1-z)^2 K_0^2(a\, r_\perp) \,\}, \end{aligned}$$

where $a^2 = z(1-z)Q^2 + m_q^2$. The functions $\Psi_{T,L}$ stand for transverse and longitudinal polarized photon wave functions. Eq. (1.1) is important since it provides a relation between the dipole-target elastic amplitude and the cross section of the diffraction dissociation. A non-linear evolution equation was derived for the former [8, 9, 10, 11, 12, 13, 14]. This equation has been studied both analytically [14, 15] and numerically [13, 16, 17, 18].

The formula (1.1) fails to describe correctly the experimental data on the diffraction production. Moreover, inclusion of an extra gluon emission in the initial virtual photon wave function is still insufficient to reproduce the data [19, 20, 21, 22]. Nevertheless, Eq. (1.1) can be viewed rather as initial condition to a more complicated equation.

The non-linear equation for the diffraction dissociation processes can be written for the amplitude N^D which has the following meaning [23].

We introduce the cross section for diffraction production with the rapidity gap larger than given $Y_0 \equiv \ln(1/x_0)$:

$$\sigma_{diff}(x, x_0, Q^2) = \int d^2 r_\perp \int dz \; P^{\gamma^*}(z, r_\perp; Q^2)\; \sigma^{diff}_{\rm dipole}(r_\perp, x, x_0)\,, \tag{1.3}$$

[1] F_D is the diffractive structure function introduced in Ref. [2].

and

$$\sigma^{diff}_{\rm dipole}(r_\perp, x, x_0) \;=\; \int d^2b\; N^D(r_\perp, x, x_0; b)\,. \tag{1.4}$$

The function N^D is the amplitude of the diffraction production induced by the dipole with size $r_\perp$ with rapidity gap larger than given (Y_0). Note that the minimal rapidity gap Y_0 can be kinematically related to the maximal diffractively produced mass: $x_0 = (Q^2 + M^2)/W^2$.

The non-linear evolution equation for N^D was derived in Ref. [23] and recently rederived in Ref. [21]:

$$N^D(\mathbf{x_{01}}, Y, Y_0; b) = N^2(\mathbf{x_{01}}, Y_0; b)\, {\rm e}^{-\frac{4C_F\,\alpha_S}{\pi}\,\ln\left(\frac{\mathbf{x_{01}}}{\rho}\right)(Y-Y_0)} \;+\; \frac{C_F\,\alpha_S}{\pi^2}\int_{Y_0}^{Y} dy\, {\rm e}^{-\frac{4C_F\,\alpha_S}{\pi}\,\ln\left(\frac{\mathbf{x_{01}}}{\rho}\right)(Y-y)}\;\times$$

$$\int_\rho d^2\mathbf{x_2}\frac{\mathbf{x_{01}^2}}{\mathbf{x_{02}^2}\,\mathbf{x_{12}^2}}[\,2\,N^D(\mathbf{x_{02}}, y, Y_0; \mathbf{b}-\frac{\mathbf{1}}{\mathbf{2}}\mathbf{x_{12}}) + N^D(\mathbf{x_{02}}, y, Y_0; \mathbf{b}-\frac{\mathbf{1}}{\mathbf{2}}\mathbf{x_{12}})N^D(\mathbf{x_{12}}, y, Y_0; \mathbf{b}-\frac{\mathbf{1}}{\mathbf{2}}\mathbf{x_{02}})$$

$$-4\,N^D(\mathbf{x_{02}}, y, Y_0; \mathbf{b}-\frac{\mathbf{1}}{\mathbf{2}}\mathbf{x_{12}})N(\mathbf{x_{12}}, y; \mathbf{b}-\frac{\mathbf{1}}{\mathbf{2}}\mathbf{x_{02}}) + 2\,N(\mathbf{x_{02}}, y; \mathbf{b}-\frac{\mathbf{1}}{\mathbf{2}}\mathbf{x_{12}})N(\mathbf{x_{12}}, y; \mathbf{b}-\frac{\mathbf{1}}{\mathbf{2}}\mathbf{x_{02}})]\,. \tag{1.5}$$

The evolution (1.5) is a subject to initial conditions at $x = x_0$:

$$N^D(r_\perp, x_0, x_0; b) \;=\; N^2(r_\perp, x_0; b)\,. \tag{1.6}$$

Namely, at the energy equal to the energy gap diffraction is purely given by the elastic scattering as it was stated in Eq. (1.1).

Since at high energies color dipoles are correct degrees of freedom [10] we can write the unitarity constraint :

$$2\,N \;=\; N^D \;+\; F\,, \tag{1.7}$$

where the function F denotes contributions of all the inelastic processes. An important observation is that F satisfies the same equation as N [11, 12] but with shifted initial conditions [23]:

$$F_{ini} \;=\; N_{ini} \;-\; N^2_{ini} \tag{1.8}$$

Another interesting quantity to study is the cross section of diffractive dissociation process with a fixed gap or equivalently to a fixed mass:

$$\Re \;\equiv\; -\partial N^D/\partial Y_0\,. \tag{1.9}$$

The function $\Re$ was introduced in Ref. [23]. The authors of this paper proposed a model in which $\Re$ was shown to possess a maximum when varying Y_0 at fixed Y. Physically this maximum means that at given Y there is a preferable mass for the production. Below we will argue that the appearance of the maximum is related to the scaling phenomena to be displayed by the function N^D.

The present paper is entirely devoted to the numerical solution of the equation (1.5). Various properties of the solutions N^D are investigated while our final goal computation of the diffraction cross section will be published separately [24]. In the next Section (2) the solution of the equation (1.5) is presented. Section 3 deals with the determination of the diffractive saturation scale. Scaling phenomena is discussed in Section 4. We conclude in the last Section (5).

2 Solution of the non-linear equation

In this section we report on the numerical solution of the equation (1.5). The method of iterations proposed in Ref. [16] is applied. The constant value for the strong coupling constant $\alpha_S = 0.25$ is always used.The solutions are computed for $4 \times 10^{-5} \leq x_0 \leq 10^{-2}$ and within the kinematic region $10^{-7} \leq x \leq x_0$ and distances up to a few fermi.

The function N^D is formally a function of four variables: the energy gap x_0, the Bjorken variable x, the transverse distance $r_\perp$, and the impact parameter b. The b-dependence is parametric only because the evolution kernel does not depend on b. In order to simplify the problem we will proceed similarly to the treatment of the b-dependence of the function N [16]. In that paper we assumed the function N to preserve the very same b-dependence as introduced in the initial conditions:

$$N(r_\perp, x; b) \; = \; (1 \; - \; e^{-\kappa(x, r_\perp)\, S(b)}), \tag{2.10}$$

with the function κ being related to the "$b = 0$" solution $\tilde{N}(r_\perp, x)$:

$$\kappa(x, r_\perp) \; = \; - \ln(1 \; - \; \tilde{N}(r_\perp, x)). \tag{2.11}$$

$\tilde{N}(r_\perp, x)$ represents a solution of the very same non-linear equation (see Refs.[11, 12]) but with no dependence on the third variable. The initial conditions for the function $\tilde{N}(r_\perp, x)$ are taken at $b = 0$. For the case of the proton target [16] the anzatz in the form (2.10) was shown to be a quite good approximation of the exact b-dependence of the solution to the non-linear equation for $N(r_\perp, x; b)$. In Ref. [17] we investigated the anzatz (2.10) for the gold target and again found it to be a very good approximation at least for impact parameters smaller than the target radius.

In order to be consistent with initial conditions (1.6) we assume the following b-dependence of N^D:

$$N^D(r_\perp, x, x_0; b) \; = \; (1 \; - \; e^{-\kappa^D(x, x_0, r_\perp)\, S(b)})^2, \tag{2.12}$$

with

$$\kappa^D(x, x_0, r_\perp) \; = \; - \ln(1 \; - \; \sqrt{\tilde{N}^D(r_\perp, x, x_0)}). \tag{2.13}$$

$\tilde{N}^D(r_\perp, x, x_0)$ represents a solution of the equation (1.5) but with no dependence on the forth variable. The initial conditions for the function $\tilde{N}^D(r_\perp, x, x_0)$ are set at $b = 0$ and $\kappa^D(x_0, x_0, r_\perp) = \kappa(x_0, r_\perp)$. Since in the present paper we do not intend to compute cross sections, for which we would need to perform the b integration, the accuracy of the anzatz (2.12) will not be investigated here.

For each initial value of x_0 the function $\tilde{N}^D(r_\perp, x, x_0)$ is obtained after about ten iterations. The Fig. 1 shows the solutions $\tilde{N}^D$ as a function of the distance for various values of x_0 and x. The amplitude for the elastic scattering $\tilde{N}^2$ [16] is plotted in the same graph. The obtained numerical inequality $\tilde{N}^2 \leq \tilde{N}^D \leq \tilde{N}$ is in perfect agreement with the physical expectations for the diffractive dissociation cross section to be larger than the elastic cross section. Another consistency check is the saturation of the function $\tilde{N}^D$ which is a consequence of the unitarity bound. In the black disk limit diffractive dissociation is a half of the total cross section.

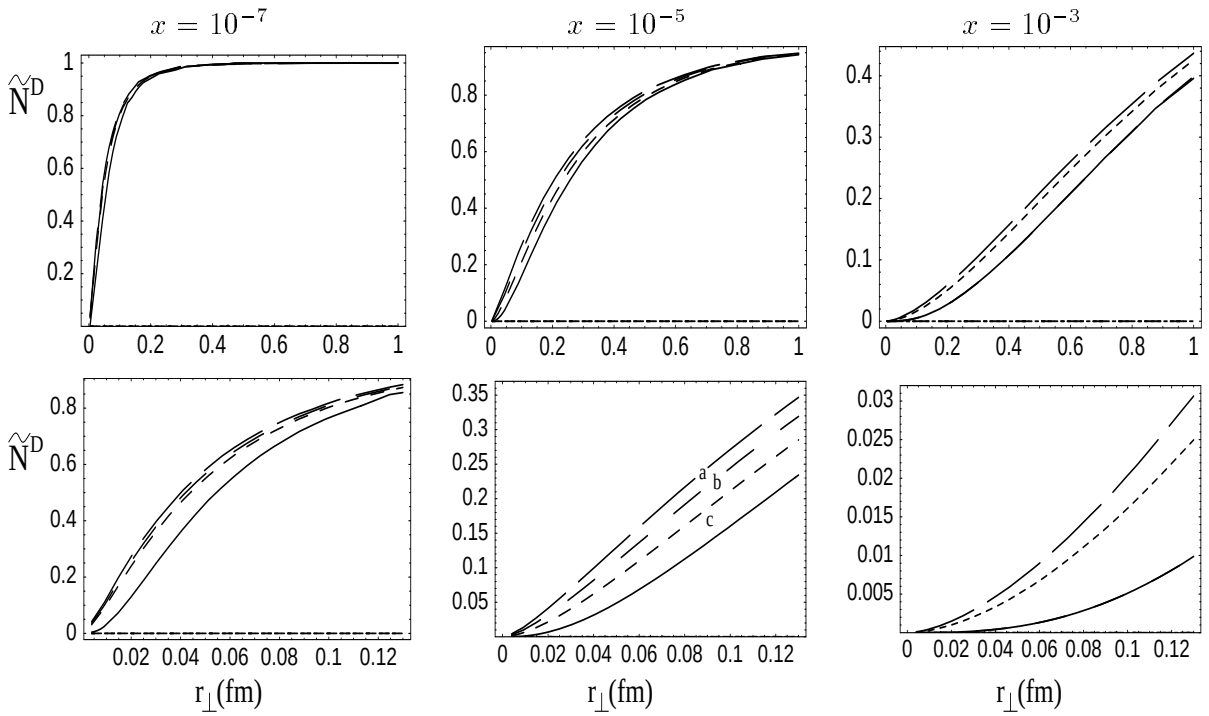

Figure 1: *The function $\tilde{N}^D$ is plotted versus distance. The curves correspond to different values of x_0: a - $x_0 = 10^{-2}$; b - $x_0 = 10^{-3}$; c - $x_0 = 10^{-4}$. The solid line is $\tilde{N}^2$.*

It is worth to investigate the dependence of the solutions obtained on the gap variable x_0. To this goal we plot the function N^D as a function of the gap Y_0 for various distances and at fixed $Y = 10$ (Fig. 2). At short distances the solution depends strongly on x_0 though as we approach the saturation region this dependence dies out.

It was stated in the Introduction that the function N^D equals $2N - F$, where both functions N and F are solutions of the same non-linear equation [11, 12]. Thus it is natural to compute $2N - F$ solving the non-linear evolution equation [11, 12] with appropriate initial conditions. A comparison with N^D from (1.5) would be an ultimate test for the correctness of the numerical procedures. Such test was successfully performed and we found an absolute agreement (relative error less than 1%) between both the computations.

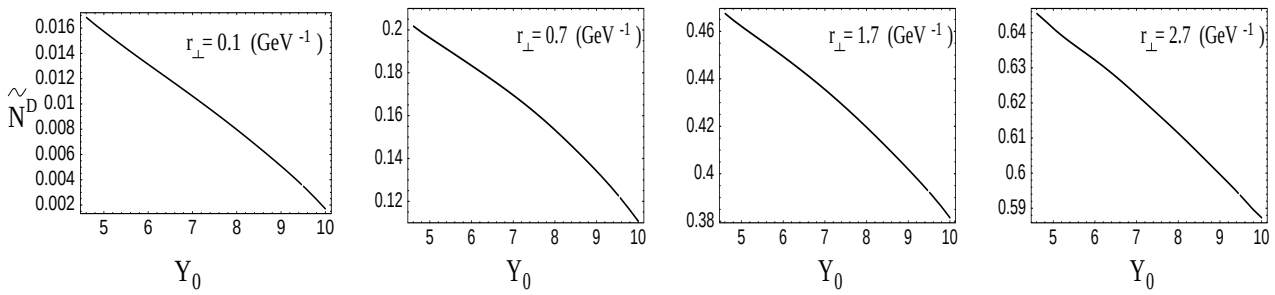

Figure 2: *The function $\tilde{N}^D$ is plotted versus the gap Y_0 at fixed rapidity $Y = 10$.*

3 Saturation Scale

Determination of the diffractive saturation scale $Q_s^D(x, x_0)$ from the solution $\tilde{N}^D$ is a subject of this section. Unfortunately, no exact mathematical definition of the saturation scale is known so far. In the Refs. [16, 25] several definitions of the saturation scale $Q_s(x)$ were proposed which related saturation scale to the shape of the function $\tilde{N}$. It is important to stress that it is not clear a priori whether Q_s^D should coincide with Q_s or not. We will proceed here in the same spirit as Ref. [25]. Namely, we propose several definitions of the saturation scale while the variety of the obtained results will indicate the uncertainty in the definitions.

For a step like function it is natural to define the saturation scale as position where it reaches half of the maximum:

- **Definition (a):**

$$\tilde{N}^D(R_s^D, x, x_0) \,=\, 1/2\,, \qquad Q_s^D \,\equiv\, 2/R_s^D\,. \tag{3.14}$$

The equality between the saturation radius R_s^D and the saturation scale Q_s^D is motivated by the double logarithmic approximation. Though this approximation is formally not justified, we still believe it to make reliable estimates provided Q_s^D is large enough. The definition (3.14) is analogous to the one proposed in Ref. [16] $N(2/Q_s, x) = 1/2$. If we recall that $N^D = N^2$ at $x = x_0$ and postulate $Q_s^D(x_0, x_0) = Q_s(x_0)$ then consistency requires

- **Definition (b):**

$$\tilde{N}^D(2/Q_s^D, x, x_0) \,=\, 1/4\,. \tag{3.15}$$

An alternative definition of the saturation scale could be one motivated by the Glauber-Mueller formula:

- **Definition (c):**

$$\kappa^D(2/Q_s^D, x, x_0) \,=\, 1/2\,. \tag{3.16}$$

The saturation scales deduced through the above definitions are depicted in Fig. 3. For given x_0 the observed hierarchy between the saturation scales obtained is an obvious consequence of

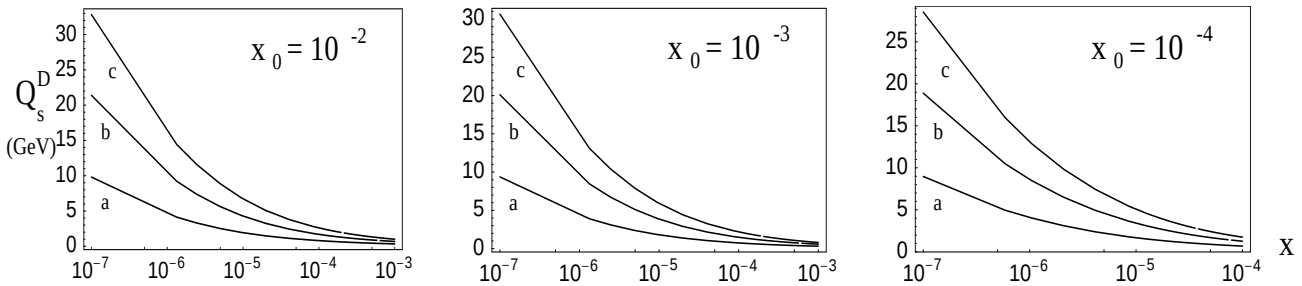

Figure 3: *The saturation scale Q_s^D is plotted versus x. The three curves correspond to the definitions (3.14) (lowest curve), (3.15) (middle curve), and (3.16) (upper curve).*

the definitions (3.14), (3.15), (3.16) and the shape of the function $\tilde{N}^D$ (Fig. 1). Note that the saturation scale is almost x_0 independent.

It is important to learn about x-dependence of the saturation scale. To this goal, we assume the following parameterization:

$$Q_s^D(x, x_0) \;=\; Q_{s\,0}^D \; x^{-\lambda} \; x_0^{\beta} \,. \tag{3.17}$$

In fact, the parameterization (3.17) is a good approximation for the values of the saturation scales obtained with

$$\lambda \;=\; 0.385 \;\pm\; 0.015\,; \quad \text{and} \quad \beta \;=\; 0.045 \;\pm\; 0.025\,.$$

Within the errors these powers coincide for all the saturation scale definitions (3.14), (3.15), (3.16). The small value for the power β is a numeric indication of the very weak x_0-dependence of the saturation scale. Its large relative error results on one hand from numerical limitations and on the other hand, this error signals for more complicated x_0-dependence than it is given in (3.17).

It is important to stress that the obtained power λ coincides with the corresponding power of the saturation scale Q_s [25].

4 Scaling phenomena

In the Ref. [25] the function $\tilde{N}$ was shown to display the scaling phenomena. We present here a similar analysis for the function $\tilde{N}^D$. In the saturation region the scaling implies the amplitude to be a function of only one variable $\tau = (r_\perp \cdot Q_s^D(x, x_0))^2$:

$$\tilde{N}^D(r_\perp, x, x_0) \;=\; \tilde{N}^D(\tau)\,. \tag{4.18}$$

Let us define the following derivative functions assuming the scaling behavior (4.18):

$$N_y^D(r_\perp, x, x_0) \;\equiv\; -\,\frac{\partial \tilde{N}^D}{\partial Y} \;=\; \frac{d\tilde{N}^D}{d\tau}\,\tau\,\frac{\partial \ln (Q_s^D)^2}{\partial \ln x}\,, \tag{4.19}$$

$$N_r^D(r_\perp, x, x_0) \equiv r_\perp^2 \frac{\partial \tilde{N}^D}{\partial r_\perp^2} = \frac{d\tilde{N}^D}{d\tau}\,\tau\,, \tag{4.20}$$

$$\Re(r_\perp, x, x_0) \equiv -\frac{\partial \tilde{N}^D}{\partial Y_0} = \frac{d\tilde{N}^D}{d\tau}\,\tau\,\frac{\partial \ln(Q_s^D)^2}{\partial \ln x_0}\,. \tag{4.21}$$

If the scaling behavior (4.18) takes place indeed, then both the ratios N_y^D/N_r^D and $\Re/N_r^D$ are $r_\perp$ independent functions. Let us first consider scaling with respect to x. Fig. 4 presents the derivatives N_y^D and N_r^D as functions of the distance $r_\perp$ at fixed $x_0 = 10^{-2}$. Both functions N_y^D

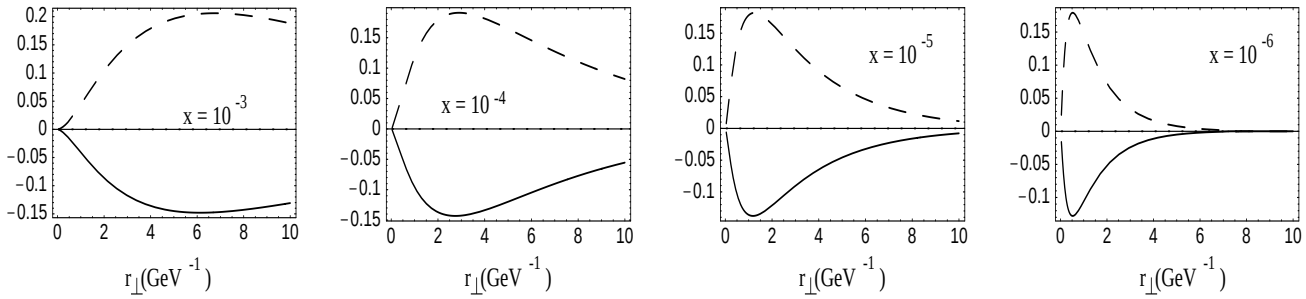

Figure 4: *The derivative functions N_r^D (dashed line) and N_y^D (solid line) as functions of the distance at fixed $x_0 = 10^{-2}$.*

and N_r^D have extrema placed at the same distance depending on x. This is a consequence of the scaling behavior (4.18) and equations (4.19) and (4.20). The extrema occur at certain τ_{max}, such that $\tilde{N}^{D\,\prime}(\tau_{max}) = -\tau_{max}\tilde{N}^{D\,\prime\prime}(\tau_{max})$. In Fig. 4, τ_{max} is approached by varying $r_\perp$ at fixed x. Alternatively it can be reached by varying x at fixed $r_\perp$ (Fig. 5).

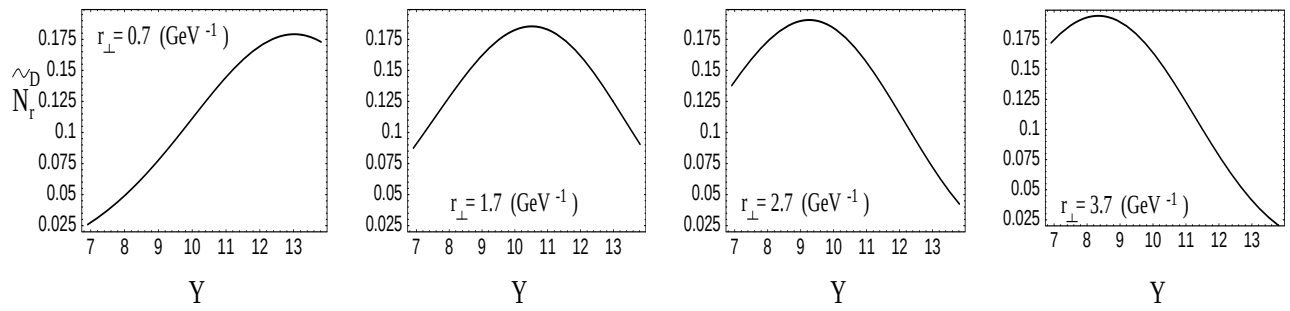

Figure 5: *The derivative function N_r^D as function of the rapidity Y at $x_0 = 10^{-2}$.*

Consider now the ratio function R_a^D:

$$R_a^D(r_\perp, x, x_0) \equiv \frac{N_y^D}{N_r^D} = \frac{\partial \ln(Q_s^D)^2}{\partial \ln x}\,. \tag{4.22}$$

If the scaling phenomenon takes place the function R_a^D is expected to be $r_\perp$ independent. We study the scaling within the distance interval $0.04\,\mathrm{GeV}^{-1} \le r_\perp \le 10\,\mathrm{GeV}^{-1}$ that corresponds to

$0.25\,\mathrm{GeV}^2 \le Q^2 \le 2.5 \times 10^3\,\mathrm{GeV}^2$. Fig. 6 presents the results on the scaling. The three lines correspond to functions N_r^D and N_y^D divided by their minimal values within the interval, and the function R_a^D multiplied by the factor 40 to be seen on the scale.

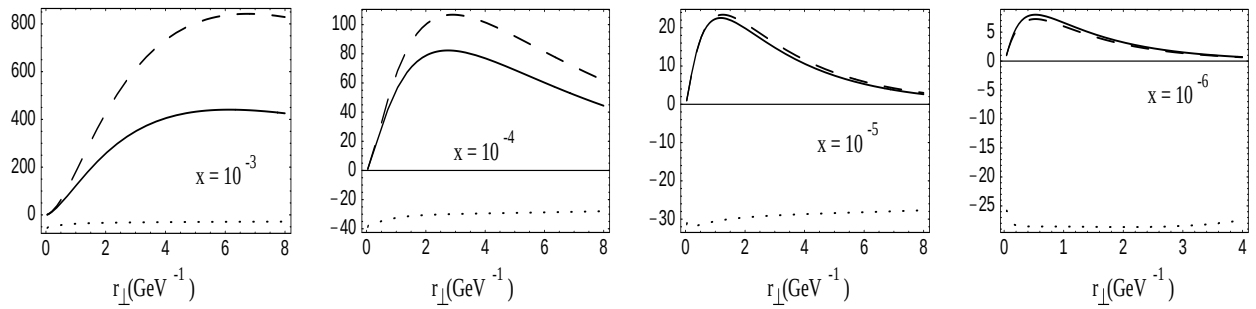

Figure 6: *The scaling as a function of the distance at fixed* $x_0 = 10^{-2}$. *The positive curves are* $N_r^D/N_{r\,min}^D$ *(dashed line) and* $N_y^D/N_{y\,min}^D$ *(solid line). The dotted line is* $40 \times R_a^D$.

The function R_a^D is clearly observed to be a very slowly varying function of $r_\perp$ for all values of x and $r_\perp$. Though at fixed x the function R_a^D cannot be claimed to be exact constant, its variations with $r_\perp$ are very much suppressed comparing to the variations of the functions N_r^D and N_y^D. For example, at $x = 10^{-5}$ within the given interval the function R_a^D changes by maximum 20%, while within the very same interval both functions N_r^D and N_y^D change in several times. Then the relative fluctuation is much less than 10%, which confirms the scaling. The phenomenon holds with a few percent accuracy and it improves at smaller $x \simeq 10^{-7}$ and in the deep saturation region. However to observe this scaling behavior in these regions is numerically more problematic since both derivatives N_r^D and N_y^D tend to zero.

The above analysis was performed for the fixed value $x_0 = 10^{-2}$. Within the errors the function $R_a^D \simeq -0.75 \pm 0.08$, constant independent on both $r_\perp$ and x. Moreover, if we repeat the same program but for different values of x_0 we discover quite similar scaling phenomena with R_a^D being numerically independent on x_0 as well. This observation implies

$$Q_s^D(x, x_0) \;=\; Q_{s\,0}^D(x_0)\, x^{-\lambda}\,; \qquad \lambda \;=\; 0.37 \;\pm\; 0.04\,. \tag{4.23}$$

Note that the value obtained for λ is in agreement with the one determined in the previous section.

Let us now study the scaling behavior with respect to the variable x_0. To this goal we investigate the function $\Re$ which is related to the x_0-dependence of the saturation scale $Q_{s\,0}^D$. Assuming $Q_{s\,0}^D \sim x_0^\beta$ we predict $\Re$ to have a maximum at $\tau = \tau_{min}$. Fig. 7 displays the function $\Re$ as a function of the distance at fixed $x = 4.54 \cdot 10^{-5}$ ($Y = 10$). In complete agreement with the scaling assumption (4.21) the function $\Re$ possesses maximum with respect to $r_\perp$ variations. The heights of the maxima are proportional to β. Since $\tau\, \tilde{N}^{D\,\prime}(\tau)|_{\tau=\tau_{max}} \simeq 0.2$, β can be estimated to be approximately 0.05 ± 0.02 which agrees with the value deduced earlier.

We can learn more about the scaling if we consider the function $\Re$ as a function of x_0 or the energy gap Y_0. In Ref. [23] a model was built in which the function $\Re$ had a maximum with respect to Y_0 variation at fixed Y. We know now that this maximum is a consequence of the scaling phenomena. The dependence of $\Re$ on Y_0 at $Y = 10$ is plotted in Fig. 8.

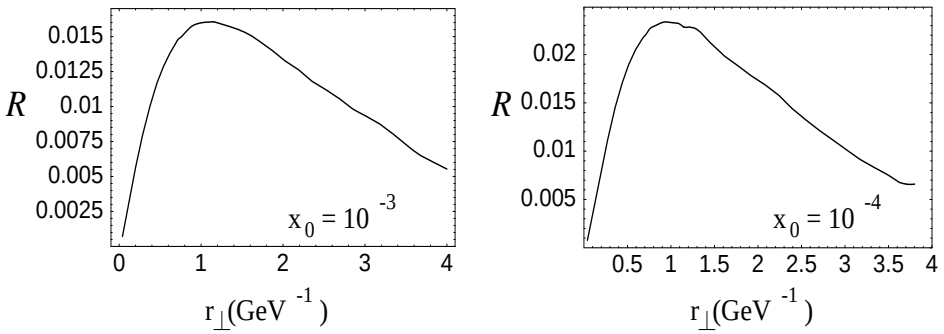

Figure 7: *The function $\Re$ versus distance at fixed $Y = 10$.*

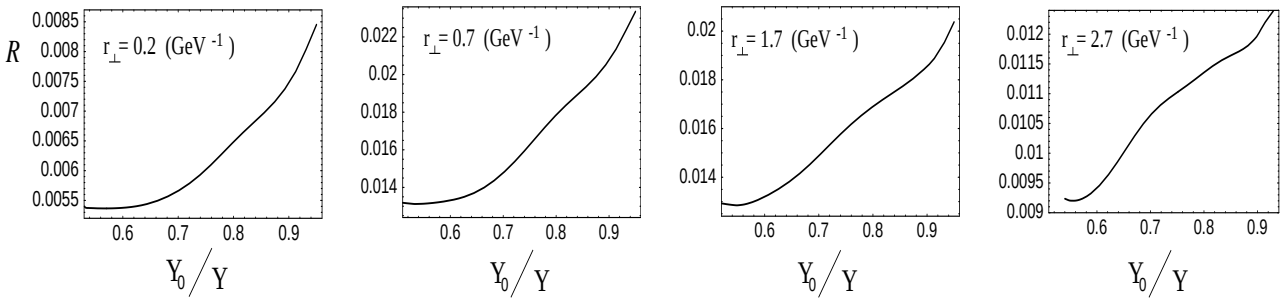

Figure 8: *The function $\Re$ as a function of the ratio Y_0/Y at fixed $Y = 10$.*

No maxima is observed on the plots of Fig. 8. In fact this is a sign of the scaling violation so far avoided by the discussion. The scaling with respect to x_0 is not exact at $Y_0 \simeq Y$. Due to its smallness ($\Re \propto \beta$) the function $\Re$ is most sensitive to small deviations from the scaling behavior:

$$\tilde{N}^D(r_\perp, x, x_0) \;=\; \tilde{N}^D_{scaling}(\tau) \;+\; \delta\tilde{N}^D(r_\perp, x, x_0) \tag{4.24}$$

In the kinematic region of the investigation variations of the function $\delta\tilde{N}^D$ with respect to $r_\perp$ and x are small compared to variations of $\tilde{N}^D_{scaling}$. In contrary, the derivative of δN^D with respect to Y_0 is of the same order as derivative of $\tilde{N}^D_{scaling}$. This is the origin of the large errors of β and the x_0 scaling violation at $x_0 \simeq x$.

In order to complete the analysis we propose yet another definition of the saturation scale based on the above presented scaling analysis. It is natural to define the saturation radius at the position where $\tau\,\tilde{N}'(\tau)$ has maximum, namely at τ_{max}:

- **Definition (d):**

$$\left(\frac{\partial\,(\tau\,\tilde{N}'(\tau))}{\partial r_\perp^2}\right)_{r_\perp^2 = 4/(Q_s^D)^2} \;=\; 0\,. \tag{4.25}$$

The saturation scale obtained from (4.25) is depicted in Fig. 9. Note again the weak dependence on the value of x_0.

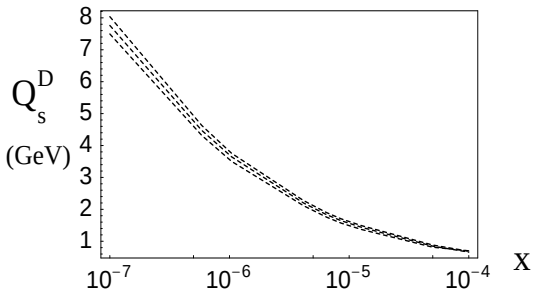

Figure 9: *The saturation scale deduced from (4.25). The different curves correspond to* $x_0 = 10^{-2}$ *(the upper curve),* 10^{-3} *(middle curve) and* $x_0 = 10^{-4}$ *(the lowest curve)*

5 Conclusions

The non-linear evolution equation (1.5) is solved numerically by the method of iterations. The solutions obtained are in agreement with the unitarity constraints: the diffraction dissociation is larger than just the elastic scattering but smaller or equal than half of the total.

The diffractive saturation scale Q_s^D is estimated form the solutions of (1.5) basing on four different definitions of the saturation scale. Though there exists a significant uncertainty in the absolute values of the scale its x-dependence is found to be the same as of Q_s - saturation scale deduced from the non-linear equation for $\tilde{N}$ [11, 12]. In fact this result is quite natural. The dependence of the saturation scale on x is entire property of the evolution equation and it should not depend on both initial conditions and saturation scale definition. The saturation scale Q_s^D is discovered to be almost independent on the minimal gap x_0.

The scaling phenomena with respect to all variables were studied in details. The scaling with respect to x is well established. It holds with a few percent accuracy in the whole kinematic region investigated. The discovered scaling should manifest itself in the experiments on diffraction, and hence it would be interesting to search for it in the $F_2^D(x, Q^2)/(Q^2\, S)$ experimental data (S stands for the target transverse area).

The numerically observed small scaling violation shows up when we consider the scaling with respect to x_0. This happens due to the weak sensitivity of the solutions to the variation of x_0. As a result, the variations of the solutions with respect to x_0 are of the same order as the scaling violation. The scaling sets in at $x \ll x_0$ but is violated at $x \sim x_0$.

The detailed analysis of the ratio between the total diffractive dissociation and the total DIS cross section will be presented in a separate publication [24]. Our preliminary computations show that this ratio happens to be independent on the central mass energy in agreement with the experimental data [2]. This independence can be traced back to the scaling property displayed by the amplitudes N and N^D and to the fact that both saturation scales depend on x with the very same power λ.

Acknowledgments

The authors are very much indebted to Jochen Bartels, Krystoff Golec-Biernat and Yuri Kovchergov for numerous helpful discussions about diffraction production in DIS. We would like to thank Asher Gotsman, Uri Maor, Eran Naftali and Kirill Tuchin for many informative and encouraging discussions. We thank DESY theory group and Hamburg University Institute of theoretical physics for their hospitality and creative atmosphere during several stages of this work.

The research of E. L. was supported in part by the BSF grant # 9800276, by GIF grant # I-620.-22.1411444 and by Israeli Science Foundation, founded by the Israeli Academy of Science and Humanities. The work of M.L. was partially supported by the Minerva Foundation and its financial help is gratefully acknowledged.

References

[1] M. Wüsthoff and A. D. Martin, *J. Phys.* **G25** (1999) R309.

[2] H1 collaboration: T. Ahmed et al., *Phys. Lett.* **B 348** (1995) 681;
ZEUS collaboration: J. Breitweg et al., *Eur. Phys. J.* **C 6** (1999) 43.

[3] E. Levin and M. Wusthoff, *Phys. Rev.* **D 50** (1994) 4306.

[4] V. A. Abramovsky, V. N. Gribov and O. V. Kancheli, Pomeron Exchange," *Yad. Fiz.* **18** (1973) 595 [*Sov. J. Nucl. Phys.* **18** (1973) 308].

[5] Y. V. Kovchegov and L. McLerran, *Phys. Rev.* **D 60** (1999) 054025, Erratum-ibid. **D 62** (1999) 019901.

[6] A. H. Mueller: *Nucl. Phys.* **B335** (1990) 115.

[7] N.N.Nikolaev and B.G. Zakharov, *Z. Phys.* **C49** (1991) 607, *Phys. Lett.* **B260** (1991) 414; E. Levin and M. Wüsthoff, *Phys. Rev.* **D50** (1994) 4306; E. Levin, A.D. Martin, M.G. Ryskin and T. Teubner, *Z. Phys.* **C74** (1997) 671.

[8] L. V. Gribov, E. M. Levin, and M. G. Ryskin, *Phys. Rep.* **100** (1981) 1.

[9] A. H. Mueller and J. Qiu, *Nucl. Phys.* **B 268** (1986) 427.

[10] A. H. Mueller, *Nucl. Phys.* **B 415** (1994) 373.

[11] Ia. Balitsky, *Nucl. Phys.* **B 463** (1996) 99.

[12] Yu. Kovchegov, *Phys. Rev.* **D 60** (2000) 034008.

[13] M. Braun, *Eur. Phys. J.* **C 16** (2000) 337, `hep-ph/0101070`.

[14] E. Iancu, A. Leonidov, and L. McLerran, hep-ph/0011241; E. Iancu and L. McLerran, *Phys. Lett.* **B 510** (2001) 145.

[15] Yu. Kovchegov, *Phys. Rev.* **D 61** (2000) 074018; E. Levin and K. Tuchin, *Nucl. Phys.* **B 573** (2000) 833; hep-ph/01012175; *Nucl. Phys.* **A 691** (2001) 779.

[16] M. Lublinsky, E. Gotsman, E. Levin, and U. Maor, hep-ph/0102321, *Nucl. Phys.* **A** (in press).

[17] E. Levin and M. Lublinsky, hep-ph/0104108, *Nucl. Phys.* **A** (in press).

[18] N. Armesto and M. Braun, *Eur. Phys. J.* **C 20** (2001) 517.

[19] E. Gotsman, E. Levin, M. Lublinsky, U. Maor and K. Tuchin, hep-ph/0007261, *Nucl. Phys.* **A** (in press).

[20] B. Z. Kopeliovich, I. K. Potashnikova, B. Povh and E. Predazzi, *Phys. Rev.* **D 63** (2001) 054001.

[21] A. Kovner and U. A. Wiedemann, hep-ph/0106240.

[22] Y. V. Kovchegov, hep-ph/0107256.

[23] Yu. Kovchegov and E. Levin, *Nucl. Phys.* **B 577** (2000) 221.

[24] E. Levin and M. Lublinsky, in preparation.

[25] M. Lublinsky, hep-ph/0106112, *Eur. Phys. J.* **C** (in press).